



Disturbance Speed Measurements in a Circular Jet via Double Focused Laser Differential Interferometry

Joseph S. Jewell*

U.S. Air Force Research Laboratory and Spectral Energies, LLC, Wright-Patterson AFB, OH 45433, USA

Ahsan Hameed[†] and Nicholaus J. Parziale[‡]

Stevens Institute of Technology, Hoboken, NJ 07030, USA

Sivaram Gogineni[§]

Spectral Energies, LLC, Beavercreek, OH 45430, USA

Measurements and calculations of the phase speed of disturbances observed in turbulent jets of three diameters are made at speeds between 80 m/s and 300 m/s, via cross-correlation of signals from a double focused laser differential interferometer (D-FLDI). A consistent trend in correlation-derived disturbance propagation speeds is observed with varying jet velocity, and the strength of the correlation decreases as the jet is moved laterally through the interferometer away from the focus point. The correlation curves also collapse across varying jet velocities when normalized. The dual FLDI beams are imaged and separation distances characterized using a beam profiler. Spectral density curves from the D-FLDI and hotwire anemometer at similar locations are compared. The effect of orienting FLDI bundles parallel with and at a 45° angle to the mean flow direction is assessed and shown to be minimal in terms of the disturbance velocity computed via cross-correlation.

I. Introduction

In the study of hypersonic boundary-layer instability, recent research has focused on predicting, with numerical methods, the frequency content of disturbances that are measured over simple geometries. The motivation for these efforts is to refine the computational predictive tools when they are applied to flowfields with the most tractable and separable problems.

To facilitate the development of boundary-layer transition prediction tools, advances in experimental methods must also keep pace. Here, we focus on the further application and development of a double focused laser differential interferometer (D-FLDI).¹ The D-FLDI is set up such that two very closely spaced probe volumes permit the accurate measurement of the phase speed or convective velocity of density disturbances in the flowfield, including in a free jet, and also potentially for hypersonic boundary-layer instability wave-packets in a hypersonic ground-test facility. This technique will ultimately enable the measurement of both phase speed and frequency content, which should serve to support improvements in predictive capabilities, as well as the assessment of free stream noise in hypersonic wind tunnels.

*Research Scientist, AFRL/RQHF, Wright-Patterson AFB, OH. jjewell@alumni.caltech.edu. AIAA Senior Member.

[†]Graduate Student, Mechanical Engineering, Castle Point on Hudson, Hoboken, NJ. AIAA Student Member.

[‡]Assistant Professor, Mechanical Engineering, Castle Point on Hudson, Hoboken, NJ. AIAA Senior Member.

[§]President, Spectral Energies, LLC, Beavercreek, OH. AIAA Fellow.

II. Double Focused Laser Differential Interferometry (D-FLDI)

The FLDI¹⁻⁸ is an optical technique which permits the high-speed and non-intrusive interrogation of small-amplitude density perturbations at a small probe volume. In Smeets,⁴ Figure 3 depicts the use of a Koester prism (an assembly of two identical right angle prisms) to separate a single FLDI bundle into two FLDI bundles. We refer to an FLDI bundle as the two orthogonally polarized laser beams that comprise one FLDI. In this work, we also use a Koester prism and half-wave plate placed such that approximately 1/2 of the laser power is directed into each FLDI bundle. This setup results in a set of two FLDI bundles (D-FLDI) that pass through the probe volume, both of which have enough power to register sufficient SNR at a photodetector at the end of the beam path. The position and attitude of the Koester prism and half-wave plate dictate the separation distance and orientation of the bundles relative to each other. A schematic of this D-FLDI setup is presented as Figure 1 in a configuration suitable for wind-tunnel testing; most of the signal resulting from the turbulent shear layers is rejected by each FLDI bundle due to beam overlap (see Section III). In the jet experiments described in Section IV, the beam separation is 1610 μm for the double FLDI setup.

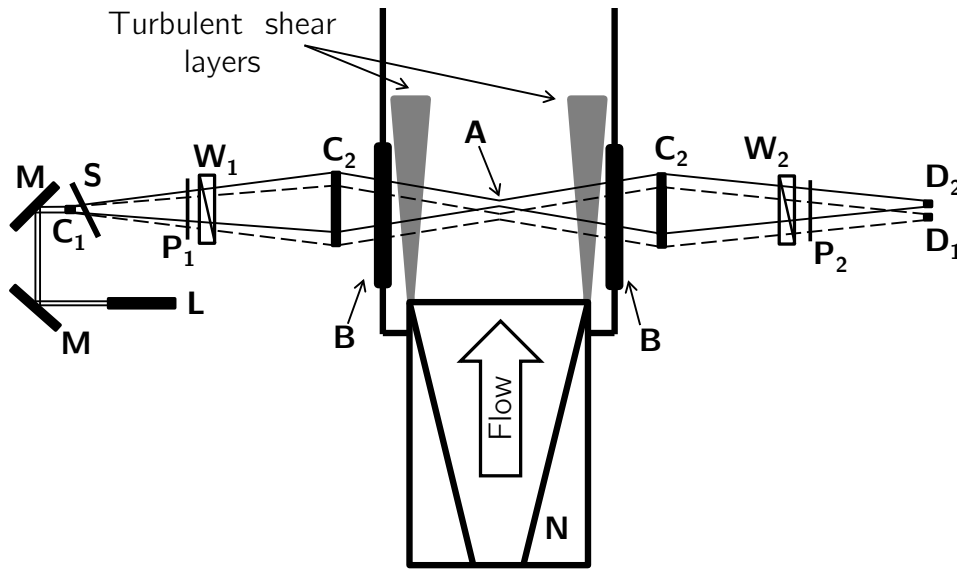


Figure 1. Annotated schematic of the FLDI in a configuration suitable for wind-tunnel testing. L, Laser; M, mirror; C₁, 10 mm focal length lens; C₂, 300 mm focal length lens; P, polarizer; W, Wollaston prism (2 arc minutes); B, BK7 window; A, probe volume; D₁ and D₂, photodetectors; S, splitter (Koester prism), N, nozzle. Solid and dashed lines are used to denote the separated FLDI bundles.

A similar setup has also been used¹ in the Caltech T5 Hypervelocity Reflected Shock Tunnel⁹ to measure disturbances in the boundary layer on a slender five degree half-angle sharp cone in one case, which was part of the test campaign described in Parziale⁵ and Jewell.^{10,11} In this case, the two FLDI bundles were displaced approximately 1000 μm from each other. More recently, a single FLDI and unfocused LDI have been used⁸ to examine disturbance spectra in a turbulent free jet, and a D-FLDI and focusing schlieren have been used¹ to examine disturbance spectra and propagation velocities in a shock tube. An unfocused LDI¹² has also been used to study supersonic blunt body receptivity.

Spatial filtering of turbulence allows the D-FLDI technique to reject unwanted signals outside the region of interest. There are two spatial filters characteristic of the D-FLDI technique: filtering due to the finite beam separation and filtering due to the finite beam width.⁷ Their effects are modeled using signal transfer functions. The signal transfer function based on finite beam separation is derived by approximating the FLDI instrument as two point-detectors separated by a distance, Δx . For two-dimensional disturbances, it is given by Schmidt¹³ as:

$$H_{\Delta x}(k) = \frac{2}{k\Delta x} \sin \left[\frac{k\Delta x}{2} \right] \quad (1)$$

The transfer function for the finite beam width is dependent on the form of the turbulent field. For a jet following a Gaussian strength profile, with a standard deviation σ_{jet} and centered at a distance along the beam relative to the best focus, z_0 , the transfer function is given by Fulghum⁷ as

$$H_{\sigma}(k) = \sqrt{\frac{2\pi^{3/2} \exp\left(-\frac{k^2}{4} \left[w_0^2 + \frac{8\lambda^2 z_0^2}{k^2 \lambda^2 \sigma_{\text{jet}}^2 + 8\pi^2 w_0^2} \right] \right)}{\sqrt{\frac{8\pi^2}{\sigma_{\text{jet}}^2} + \frac{k^2 \lambda^2}{w_0^2}}}} \quad (2)$$

where w_0 is the beam waist radius at the best focus and λ is the laser's wavelength.

The MATLAB `pwelch` function is used to generate a power spectral density (PSD) estimate of the D-FLDI signal. The `pwelch` function provides a convenient method to convert the signal from the time domain to the frequency/wavenumber domain. To reduce the noise in the generated frequency spectrum, overlapping rectangular windows are incorporated as inputs to the `pwelch` function. The density fluctuations are extracted from the D-FLDI signal in the wavenumber domain. The deconvolution of the spatial filtering is achieved by dividing the PSD of the D-FLDI signal by the system transfer functions, thus producing a PSD of the density fluctuations. Mathematically, this is represented by the following equation:

$$F\{\rho'(t)\} = \frac{\lambda}{2\pi K_{\text{GD}} \Delta x} \left[\frac{F\{\Delta\varphi\}}{H_{\Delta x}(k) H_{\sigma}(k)} \right] \quad (3)$$

where K_{GD} is the Gladstone-Dale relation and $\Delta\varphi$ represents the signal, converted from measured voltage to phase.

III. Double FLDI Beam Profile Imaging and Analysis

The geometry of the present D-FLDI beams is investigated with a Spirocon SP620U beam profiler placed at the focus. The center-to-center distance between the two FLDI bundles comprising the D-FLDI is found to be $1391 \pm 10 \mu\text{m}$, and the distance between the two beams of each individual FLDI bundle is found to be $181 \pm 5 \mu\text{m}$. Adjusting the rotational orientation of the Wollaston prisms alters the angle along which the individual FLDI bundles are split, so that each bundle may be oriented to be sensitive primarily to horizontal fluctuations, vertical fluctuations, or both. Beam profiler images from each of these configurations are presented in Figure 2. Data taken with orientations depicted in the right and left subplots, with the FLDI legs within each bundle split at 0° and 45° angles, is used for the results presented in this paper; the velocity cross-correlation is shown to not depend strongly on the bundle orientation.

Figure 3 contains beam profiler images captured off focus to demonstrate beam overlap away from the sensitive region. The two FLDI legs within each bundle overlap substantially by 20 mm away from the focus, and the bundles themselves overlap by 30 mm away.



Figure 2. *Left:* FLDI legs within each bundle split horizontally; maximally sensitive to disturbances parallel with the jet flow. *Center:* FLDI legs split vertically; maximally sensitive to disturbances transverse to the jet flow. *Right:* FLDI legs split at a 45° angle; partially sensitive to disturbances both parallel with and transverse to the jet flow.

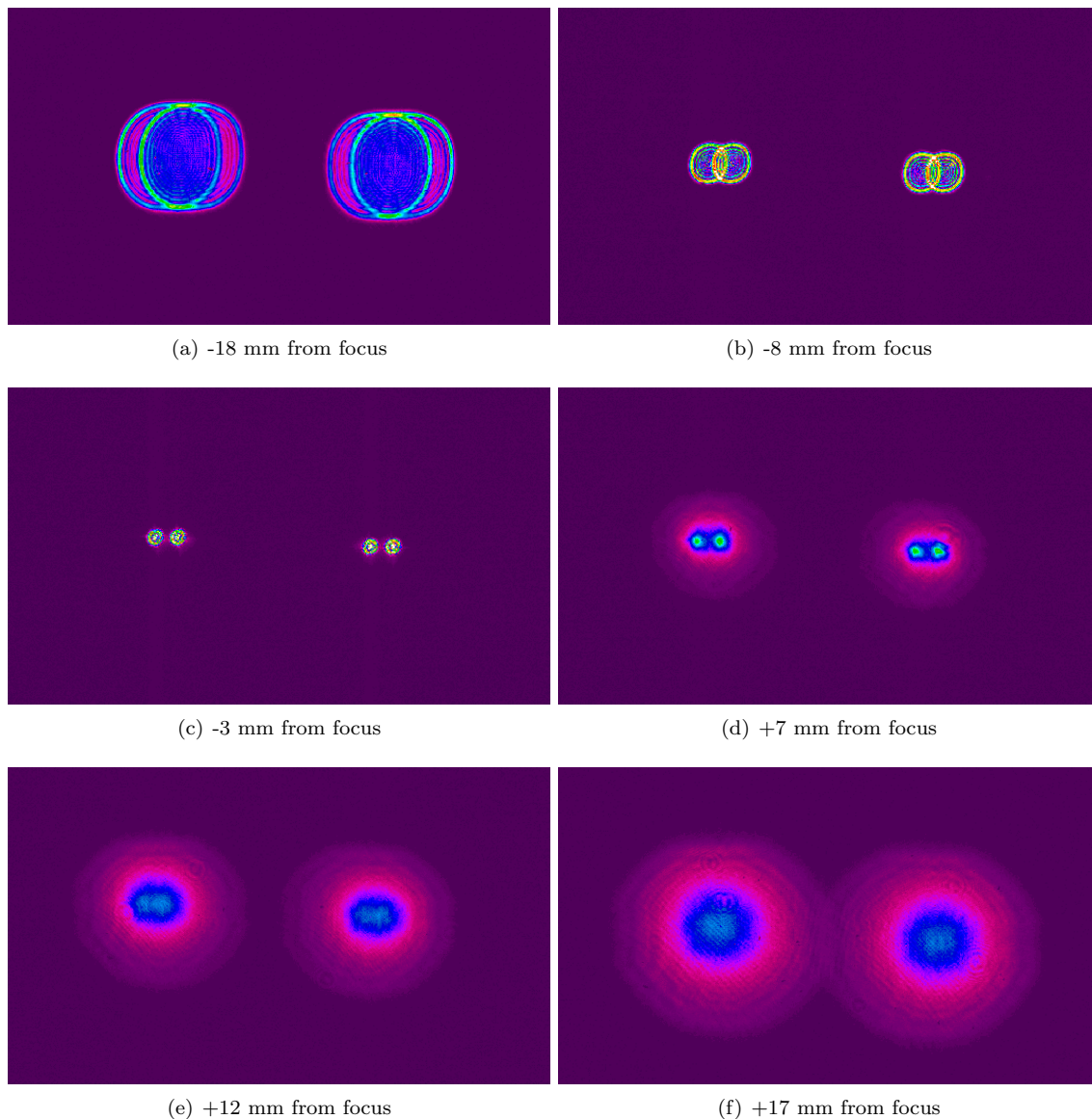


Figure 3. Beam profiler images captured off focus. The two FLDI legs within each bundle overlap substantially by 20 mm away from the focus.

IV. Free Jet Double FLDI Results

Single and double FLDI experiments, to compare FLDI-measured velocities with flowfield features of known velocity (such as disturbances in a free jet) as well as to measure phase speeds or convective velocities of disturbances with unknown velocities, are performed using a Dantec StreamLine Pro Automatic Calibrator jet at the U.S. Air Force Research Laboratory (AFRL) at Wright-Patterson Air Force Base, Ohio. The jet calibrator is comprised of a pitch-yaw-roll manipulator for controlling hotwire anemometer orientation and location in a well-characterized nozzle flow, which is capable of supplying exit velocities from 0.5 m/s to 300 m/s using three nozzles with diameters of 5.04 mm, 8.74 mm, and 12.36 mm. Where geometry allows, the D-FLDI sensitive region is positioned directly in front of the hotwire anemometer, as shown in Figure 4. A detail from the source side of the dual interferometer instrument, showing the Koester prism splitting the expanding beam into two beams with a separation of 1.61 mm, is presented in Figure 5. Sample hotwire anemometer power spectral density results from the present configuration are presented in Figure 6.

The D-FLDI output signals are measured with two ThorLabs DET36A photodetectors (25 MHz bandwidth)

amplified 25× with a SR445A 350 MHz preamplifier. Samples of 25 ms were recorded at 100 MHz for each of the two D-FLDI bundles on a Cleverscope CS320A digital oscilloscope. The recorded voltages were reduced as described in Parziale⁵ and cross correlated using the MATLAB `xcorr` function.



Figure 4. Dantec hotwire anemometer jet calibrator mounted across D-FLDI setup. The sensitive region of the FLDI (top left) is placed 2 mm in front of the hotwire anemometer.

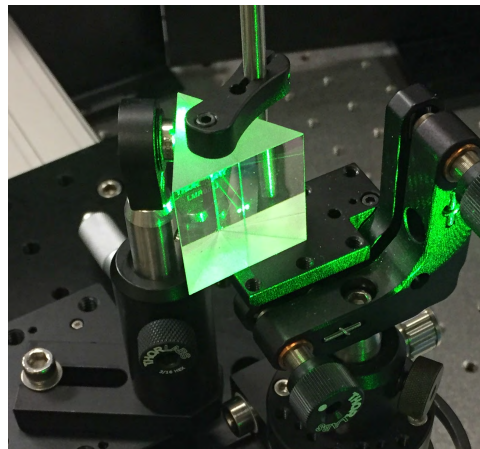


Figure 5. A Koester prism splits the expanding source beam into two beams with roughly equal power and a separation of 1.61 mm.

D-FLDI and hotwire anemometer power spectral densities are compared in Figure 8, with a $-5/3$ line for reference, for a 200 m/s jet with the HWA and the focus of the first FLDI bundle positioned 59 mm downstream of the jet exit.

A cross-correlation of double FLDI signals was performed for several experiments with the 5.04 mm diameter free jet at velocities ranging from 50 to 300 m/s. An example of these cross-correlated results, which are used together with the measured beam separation of 1.61 mm to calculate disturbance velocities, are presented in Figure 7 for a 250 m/s experiment. The correlation curve between the two signals is fitted with a polynomial of degree six (in red), and the lag measured from the peak (red circle) of this curve. The lag between the two signals for this case is 7.76 μ s, which implies a disturbance velocity of 207.5 m/s, which is 83% of the jet velocity.

Figure 9 presents D-FLDI peak cross-correlation velocities as a function of free jet velocity for the 5.04 mm diameter case, from FLDI bundle orientations of both 0° and 45° . The velocity cross-correlation does not

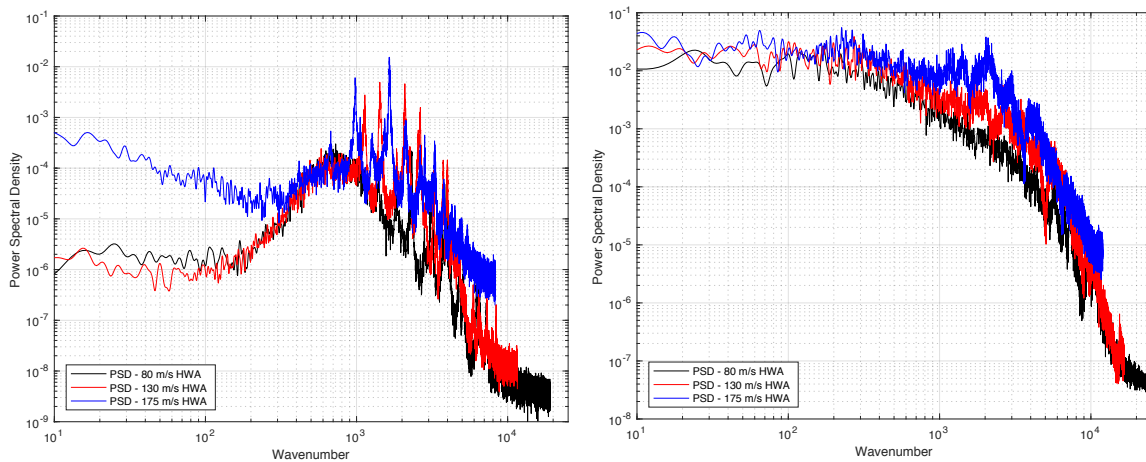


Figure 6. Single-wire hotwire anemometer results for three jet velocities, at two different distances from the Dantec StreamLine Pro Automatic Calibrator jet exit: 0 mm from the nozzle exit (left) and 43 mm from the nozzle exit (right).

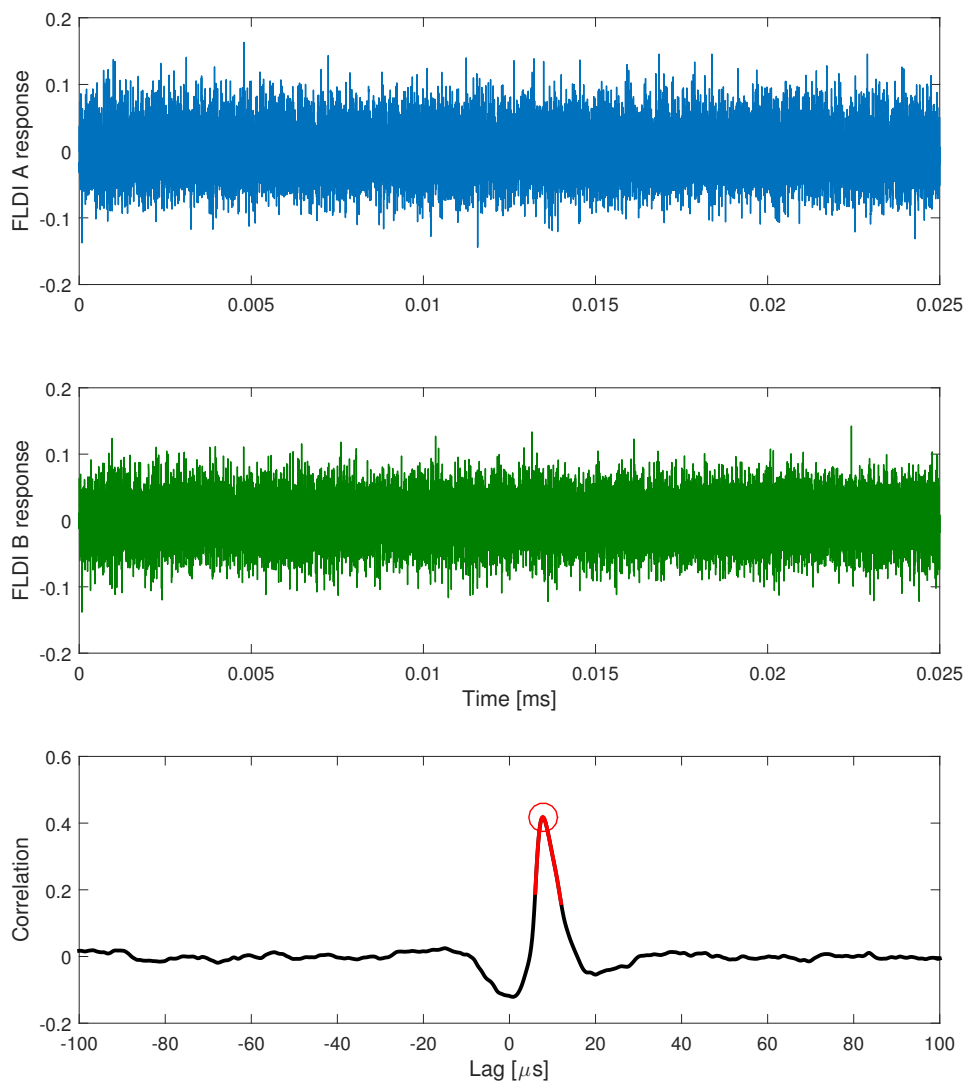


Figure 7. Cross-correlation of double FLDI signals for a 5.04 mm diameter free jet at 250 m/s, with the D-FLDI sensitive region centered on the jet and placed 7.5 mm from the exit.

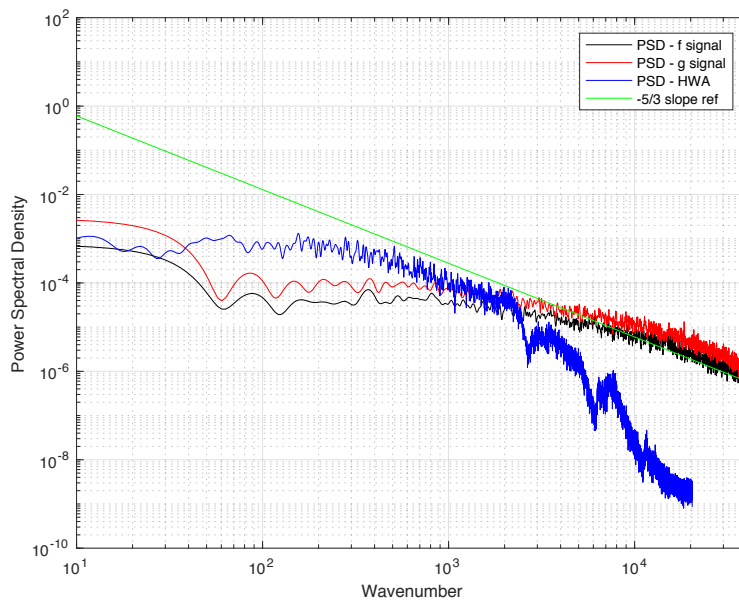


Figure 8. HWA (blue) and D-FLDI (black and red) power spectral densities compared, with a $-5/3$ line (green) for reference, for a 200 m/s jet with the HWA and the focus of the first FLDI bundle positioned 59 mm downstream of the jet exit. The PSDs overlap for wavenumbers from approximately 1000 to 2200, after which the HWA signal rolls off and the two FLDI signals continue along the $-5/3$ reference line.

depend on the bundle orientation. Reynolds numbers based on jet exit diameter ranged from 1.70×10^4 (for the 50 m/s case) to 1.04×10^5 (for the 300 m/s case). The measured disturbance velocities were between 65% and 85% of the nominal jet velocities from the Dantec calibrator apparatus.

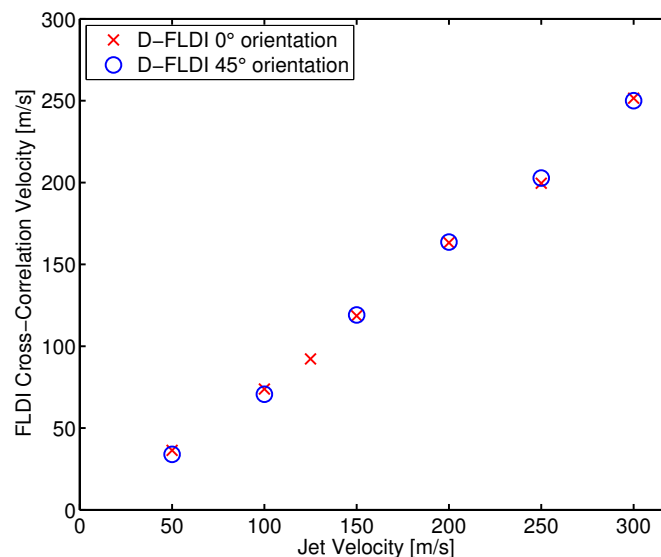


Figure 9. D-FLDI peak cross-correlation velocities as a function of free jet velocity for the 5.04 mm diameter case. The D-FLDI sensitive region is centered on the jet exit, 7.5 mm downstream. Results from FLDI bundle orientations of both 0° and 45° are presented; the velocity cross-correlation does not depend on the bundle orientation.

The jet, held at constant values of 150, 200, 250 and 300 m/s and 7.5 mm upstream from the first FLDI beam, was traversed laterally with an electronically-actuated stage through the D-FLDI beams from the focus (emphie.e., the most sensitive region) to about 150 mm away from the focal point. Cross correlations were attempted on the two FLDI beams at the focus and several locations away from the focus. The output of the MATLAB `xcorr` function for these locations is presented in Figure 10. The correlation peak is strongest at the focus, has dropped by more than 80% by 30 mm away from the focus, and is nearly zero by 90 mm away from the focus. For this jet diameter and D-FLDI geometry, the D-FLDI cross correlation provides

a disturbance velocity measurement which is most sensitive at the focus and insensitive more than a few centimeters away from the focus. In future work, additional cases with varying jet diameter will be used to further extend or limit this conclusion.

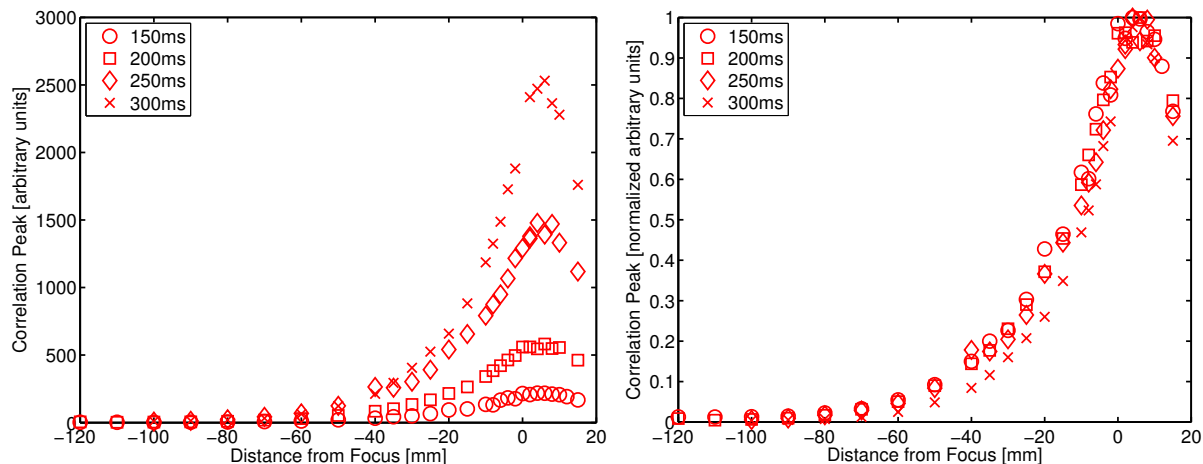


Figure 10. D-FLDI peak cross-correlation values as a function of lateral displacement from the D-FLDI sensitive region for the 5.04 mm diameter case for four different velocities (left), which collapse when normalized (right).

V. Future Work

In future work, further spectral density curves from the double FLDI and hotwire anemometer at similar locations will be compared with each other, the effect of orienting FLDI bundles parallel and perpendicular to the mean flow direction will be assessed, and dispersion characteristics will be discussed. Error estimates, particularly on the velocity measurements, will also be made. The disturbance propagation velocity measurements will be compared with theoretical and measured values for convective velocity in round jets from the literature.^{14–19}

Further work with the dual-beam FLDI apparatus will be pursued as part of a series of experiments²⁰ on a slender 7-degree half-angle cone of variable bluntness, similar to the work performed with an 8-degree cone by Stetson²¹ and recently analyzed by Jewell and Kimmel.²² For this test campaign, possible variable phase speed within individual wave packets will be examined and the performance of the double FLDI sensor over a wider range of hypersonic-tunnel-relevant conditions will be ascertained. Complementary computations of the flowfield and stability properties of these experiments are also planned.

Acknowledgments

This research was performed under Air Force Phase I SBIR SB1711-001-1 “Non-intrusive measurement of density and velocity perturbations in supersonic and hypersonic wind tunnels”, managed by Eric Marineau of AEDC. The authors thank Ethan Legge, Stephen Grib and Tim Erdman of Spectral Energies for assistance with the hotwire anemometer and jet apparatus, Paul Hsu and Naibo Jiang of Spectral Energies for assistance with optics, and Roger Kimmel of AFRL for advice and consultation.

References

- ¹Jewell, J. S., Parziale, N. J., Lam, K.-Y., Hagen, B. J., and Kimmel, R. L., “Disturbance and Phase Speed Measurements for Shock Tubes and Hypersonic Boundary-Layer Instability,” *AIAA Aviation 2016*, AIAA-2016-3112, Washington, DC, 2016. doi: 10.2514/6.2016-3112.
- ²Smeets, G., “Laser Interferometer for High Sensitivity Measurements on Transient Phase Objects,” *IEEE Transactions on Aerospace and Electronic Systems*, Vol. AES-8, No. 2, 1972, pp. 186–190. doi: 10.1109/TAES.1972.309488.
- ³Smeets, G., “Laser-Interferometer mit grossen, fokussierten Lichtbündeln für lokale Messungen,” ISL - N 11/73, 1973.
- ⁴Smeets, G., “Verwendung eines Laser-Differentialinterferometers zur Bestimmung lokaler Schwankungsgrößen sowie des mit-

tlere Dichteprofile in einem turbulenten Freistrahle,” ISL - N 20/74, 1974.

⁵Parziale, N. J., *Slender-Body Hypervelocity Boundary-Layer Instability*, Ph.D. thesis, [California Institute of Technology](#), Pasadena, CA, 2013.

⁶Parziale, N. J., Shepherd, J. E., and Hornung, H. G., “Free-stream density perturbations in a reflected-shock tunnel,” *Experiments in Fluids*, Vol. 55, No. 2, 2014, pp. 1–10. doi: [10.1007/s00348-014-1665-0](#).

⁷Fulghum, M. R., *Turbulence measurements in high-speed wind tunnels using focusing laser differential interferometry*, Ph.D. thesis, The Pennsylvania State University, 2014.

⁸Ceruzzi, A. P. and Cadou, C. P., “Turbulent Air Jet Investigation using Focused Laser Differential Interferometry,” *AIAA Aviation 2017*, AIAA-2017-4834, Denver, CO, 2017. doi: [10.2514/6.2017-4834](#).

⁹Hornung, H. G., “Performance Data of the New Free-Piston Shock Tunnel at GALCIT,” *Proceedings of 17th AIAA Aerospace Ground Testing Conference*, AIAA, Nashville, TN, 1992. doi: [10.2514/6.1992-3943](#), AIAA-1992-3943.

¹⁰Jewell, J. S., *Boundary-Layer Transition on a Slender Cone in Hypervelocity Flow with Real Gas Effects*, Ph.D. thesis, [California Institute of Technology](#), Pasadena, CA, 2014.

¹¹Jewell, J. S. and Shepherd, J. E., “T5 Conditions Report: Shots 2526–2823,” Tech. rep., California Institute of Technology, Pasadena, CA, June 2014, [GALCIT Report FM2014.002](#).

¹²Salzer, T. R., Collicott, S. H., and Schneider, S. P., “Feedback Stabilized Laser Differential Interferometry for Supersonic Blunt Body Receptivity Experiments,” *Proceedings of 38th Aerospace Sciences Meeting and Exhibit*, AIAA-2000-0416, Reno, NV, 2000. doi: [10.2514/6.2000-416](#).

¹³Schmidt, B. E. and Shepherd, J. E., “Analysis of Focused Laser Differential Interferometry,” *Applied Optics*, Vol. 54, 10 2015, pp. 8459. doi: [10.1364/AO.54.008459](#).

¹⁴Russ, S. and Strykowski, P. J., “Turbulent structure and entrainment in heated jets: The effect of initial conditions,” *Physics of Fluids A*, Vol. 5, No. 12, 1993, pp. 3216–3225. doi: [10.1063/1.858678](#).

¹⁵Lau, J. C., Morris, P. J., and Fisher, M. J., “Measurements in subsonic and supersonic free jets using a laser velocimeter,” *Journal of Fluid Mechanics*, Vol. 93, 1979, pp. 1–27. doi: [10.1017/S0022112079001750](#).

¹⁶Tinney, C. E., Glauser, M. N., and Ukeiley, L. S., “Low-dimensional characteristics of a transonic jet. Part 1. Proper orthogonal decomposition,” *Journal of Fluid Mechanics*, Vol. 612, 20028, pp. 107–141. doi: [10.1017/S0022112008002978](#).

¹⁷Wernet, M. P., “Temporally resolved PIV for spacetime correlations in both cold and hot jet flows,” *Measurement Science and Technology*, Vol. 18, No. 5, 2007, pp. 1387–1403. doi: [10.1088/0957-0233/18/5/027](#).

¹⁸Fleury, V., Bailly, C., Jondeau, E., Michard, M., and Juvé, D., “SpaceTime Correlations in Two Subsonic Jets Using Dual Particle Image Velocimetry Measurements,” *AIAA Journal*, Vol. 46, No. 10, 2008, pp. 2498–2509. doi: [10.2514/1.35561](#).

¹⁹Thurow, B. S., *On the convective velocity of large-scale structures in compressible axisymmetric jets*, Ph.D. thesis, The Ohio State University, Columbus, OH, 2005.

²⁰Jewell, J. S., Kennedy, R. E., Laurence, S. J., and Kimmel, R. L., “Transition on a Variable Bluntness 7-Degree Cone at High Reynolds Number,” *AIAA SciTech 2018*, AIAA-2018-1822, Kissimmee, FL, 2018. doi: [10.2514/6.2018-1822](#).

²¹Stetson, K. F., “Nosetip Bluntness Effects on Cone Frustum Boundary Layer Transition in Hypersonic Flow,” *Proceedings of the AIAA 16th Fluid and Plasma Dynamics Conference*, AIAA-1983-1763, Danvers, Massachusetts, 1983. doi: [10.2514/6.1983-1763](#).

²²Jewell, J. S. and Kimmel, R. L., “Boundary Layer Stability Analysis for Stetsons Mach 6 Blunt Cone Experiments,” *Journal of Spacecraft and Rockets*, Vol. 54, No. 1, 2017, pp. 258–265. doi: [10.2514/1.A33619](#).